Translational Oncology 37 (2023) 101755

Contents lists available at ScienceDirect

Translational Oncology

journal homepage: www.elsevier.com/locate/tranon

Original Research

MiR-196b-5p activates NF-κB signaling in non-small cell lung cancer by directly targeting NFKBIA

Wangyu Zhu [a,b,1], Yun Yu [a,b,1], Yuxin Ye [b], Xinyue Tu [b], Yan Zhang [b,c], Tao Wu [b], Lianli Ni [b], Xiangjie Huang [b], Yumin Wang [c,**], Ri Cui [a,b,*]

[a] Cellular and Molecular Biology Laboratory, Affiliated Zhoushan Hospital of Wenzhou Medical University, Zhoushan, Zhejiang 316020, China
[b] Cancer and Anticancer Drug Research Center, School of Pharmaceutical Sciences, Wenzhou Medical University, Wenzhou, Zhejiang 325035, China
[c] Key Laboratory of Clinical Laboratory Diagnosis and Translational Research of Zhejiang Province, The First Affiliated Hospital of Wenzhou Medical University, Wenzhou, Zhejiang 325000, China

ARTICLE INFO

Keywords:
miR-196b-5p
NSCLC
NFKBIA
NF-κB
STAT3
IL-6

ABSTRACT

Background: Our recent study found that QKI-5 regulated miRNA, miR-196b-5p, promotes non-small cell lung cancer (NSCLC) progression by directly targeting GATA6, TSPAN12 and FAS. However, the biological functions of miR-196b-5p in NSCLC progression and metastasis still remain elusive.

Methods: Cell proliferation, migration, colony formation, cell cycle assays were used to investigate cellular phenotypic changes. Quantitative real-time PCR (qRT-PCR) and western blot analyses were used to measure expressions of relative gene and protein. Interaction between QKI-5 and miR-196b-5p was determined by RNA immunoprecipitation (RIP) assay. Luciferase reporter assay was used to determine direct binding between miR-196b-5p and NFKBIA 3′-UTR. ELISA assay was used to measure secreted IL6 proteins. Mice xenograft model was used to assess the functions of NFKBIA on *in vivo* tumor growth.

Results: We demonstrated that the miR-196b-5p facilitates lung cancer cell proliferation, migration, colony formation, and cell cycle by directly targeting NFKBIA, a negative regulator of NFκB signaling. Knocking down NFKBIA increases IL6 mediated phosphorylation of signal transducer and activator of transcription 3 (STAT3) to promote lung cancer cell growth by activating NFκB signaling. The expression of NFKBIA was significantly downregulated in NSCLC tissue samples, and was negatively correlated with the expression miR-196b-5p. In addition, we found that downregulated QKI-5 expression was associated with the elevated miR-224 expression in NSCLC.

Conclusions: Our findings indicated that the miR-224/QKI-5/miR-196b-5p/NFKBIA signaling pathway might play important functions in the progression of NSCLC, and suggested that targeting this pathway might be an effective therapeutic strategy in treating NSCLC.

Introduction

Lung cancer is a leading cause of cancer related death worldwide. NSCLC is a major lung cancer type, and accounts for approximately 80%−85% of all lung cancer cases [1,2]. Despite recent advancements in molecular targeted therapies and immunotherapies targeting the disease, the 5-year survival rate is very poor [3]. Thus, identifying novel molecular targets is urgently required for NSCLC.

MiRNAs are small non-coding RNAs implicated in cancer progression and metastasis [4]. They function by negatively regulating target mRNA stability and/or suppressing mRNA translational processes by targeting complementary sequences in the 3′-untranslated regions (UTRs) of target genes [5]. Several studies reported miRNAs are widely involved in NSCLC progression and metastasis. In late stage disease, elevated miR-21 expression was frequently observed and associated with metastasis, and promoted cell proliferation and invasion by inhibiting

* Corresponding author: Cancer and Anticancer Drug Research Center, School of Pharmaceutical Sciences, Wenzhou Medical University, Wenzhou, Zhejiang 325035, China.
** Corresponding author at: Key Laboratory of Clinical Laboratory Diagnosis and Translational Research of Zhejiang Province, The First Affiliated Hospital of Wenzhou Medical University, Wenzhou, Zhejiang 325000, China
E-mail addresses: wym0577@163.com (Y. Wang), wzmucuiri@163.com (R. Cui).
[1] These authors contributed equally to this work.

https://doi.org/10.1016/j.tranon.2023.101755
Received 6 May 2023; Received in revised form 6 July 2023; Accepted 2 August 2023

the tumor suppressor PTEN in NSCLC [6,7]. Additionally, miR-19b facilitated NSCLC tumor growth by targeting PPP2R5E and BCL2L11 [8], while miR-200 sensitized the KRAS mutant NSCLC cells to the MEK inhibitor by suppressing ZEB1 [9] and inhibiting lung cancer cell invasion and metastasis by targeting the epithelial-mesenchymal transition (EMT) inducer, Foxf2 [10]. MiR-34a is a proapoptotic transcriptional target of p53 and directly targeted and inhibited PDL1 expression in NSCLC cells. The treatment of a syngeneic lung cancer mouse model with MRX34, a liposomal formulation complexed with miR-34a mimics, alone or in combination with radiotherapy inhibited PDL1 expression in tumors and antagonized T-cell exhaustion [11]. A phase 1 clinical study of MRX34 validated its manageable toxicity and the dose-dependent suppression of related target genes in advanced solid tumors, including lung cancer, suggesting that targeting miRNAs could be a promising therapeutic anti-cancer strategy [12].

NF-κB signaling has critical functions during cell apoptosis and proliferation. NF-κB inhibits cell apoptosis by inducing anti-apoptotic factors, including cellular inhibitors of apoptosis (cIAPs), FADD (FAS associated death domain)-like IL-1β-converting enzyme (FLICE) inhibitory protein (c-FLIP), and BCL2 proteins [13]. In addition, NF-κB facilitates cell cycle progression by transcriptionally regulating genes involved in cell cycle machinery, including cyclin D1, D2, D3 and E [14]. NFKBIA (IkBα) is a member of the inhibitors of NF-kB (IkBs) (IkBα, IkBβ, IkBε and Bcl-3) that interacts with RDH domains in NF-κB proteins and inactivates NF-κB signaling [15]. Defective NFKBIA is frequently observed in several solid tumors including breast, colon, ovarian, pancreatic, bladder, and prostate cancer [16]. NFKBIA inhibits NF-κB signaling by competitively binding to the nuclear localization signals (NLS) in NF-κB protein, and retaining it in an inactive state in the cytoplasm [17].

Recently, we reported that the RNA binding protein, QKI-5, was down-regulated in NSCLC tissue and exerted tumor suppressive functions by negatively regulating miR-196b-5p. Up-regulated miR-196b-5p promoted NSCLC progression and metastasis by inhibiting the tumor suppressor, GATA6, TSPAN12, and FAS [18,19]. However, the underlying molecular mechanisms of miR-196b-5p in NSCLC remain elusive.

In the present study, we found that NFKBIA, a negative regulator of NF-κB, is a direct target of miR-196b-5p. The expression of *NFKBIA* was down-regulated in NSCLC and anti-correlated with miR-196b-5p expression. Knocking down NFKBIA promoted lung cancer cell growth via NF-κB/IL-6-mediated STAT3 activation. We also demonstrated that the miR-224 inhibited QKI-5 expression in NSCLC. Therefore, our insights on the miR-224/QKI-5/miR-196b/NFKBIA axis could provide better therapeutic strategies for NSCLC.

Materials and methods

Cell culture and reagents

Pre-miR-196b precursor (PM12946), pre-miR-224 precursor (PM15149) and pre-miR negative control#1 (AM17110) were purchased from ThermoFisher. The miR-196b inhibitor and negative control were purchased from GenePharma (Shanghai, China). pLightSwtich empty, NFKBIA-3′UTR vectors were ordered from Active Motif. Mutations were generated by using the QuickChange II XL Site-Directed Mutagenesis Kit (Stratagene). siRNA negative control (SIC001), siQKI-5 (SASI_Hs01_00227029), shRNA control (SHC001), shNFKBIA (TRCN0000355914) were purchased from Sigma. The human lung cancer cell lines (A549 and H1299) were purchased from the American Type Culture Collection (ATCC) and were cultured in RPMI-1640 medium (Gibco, Eggenstein, Germany) supplemented with 10% heat-inactivated fetal bovine serum (Gibco) and 100 U/mL penicillin-streptomycin (Gibco, Carlsbad, CA, USA). 293T cells were cultured in DMEM medium supplemented with 10% FBS and 100 U/mL penicillin-streptomycin. All the cells were cultured in a humidified incubator with 5% CO_2 at 37 °C. Cell Cycle Regulation Antibody Sampler Kit (9932T), antibodies against pSTAT3 (9145S), STAT3 (12640S), NFKBIA (4814), GAPDH (5174S), HRP-conjugated secondary antibodies (7074) were purchased from Cell Signaling Technology (Danvers, USA). Antibody against Lamin B1 (12,987–1-AP) was obtained from proteintech (Wuhan, China). Anti-p65 (sc-9008) was purchased from Santa Cruz Biotechnology (Santa Cruz, USA). Antibodies against Ki67 (ab16667), CD31 (ab28364), and QKI-5 (ab232502) were purchased from Abcam (Cambridge, USA). Rabbit secondary antibody conjugated with horseradish peroxidase (ready to use, PV-6001) was purchased from ZSGB-BIO (Beijing, China). Human IL-6 Uncoated ELISA Kit (88–7066) was obtained from Invitrogen (Invitrogen, USA). 3-(4, 5-dimethyl thiazol-2-yl)−2, 5-diphenyl tetrazolium bromide (MTT) was manufactured from Solarbio (Beijing, China).

Gene knockdown

The pre-miR-196b precursor, pre-miR-224 precursor, pre-miR negative control, siRNA control and siQKI-5 were transfected into the lung cancer cells by Lipofectamine 3000 (Invitrogen, Carlsbad, CA, USA) reagents according to the manufacturer's instructions. The transfection of shRNAs against NFKBIA and control vector were performed with Lipofectamine 3000 regents according to the manufacturer's instructions. The successfully transfected cells were selected with 2 μg/mL puromycin (Invitrogen, USA) for 7–10 days and continued to culture in RPMI-1640 medium containing with 10% FBS and 2 μg/mL puromycin.

Quantitative real-time PCR (qRT-PCR)

We extracted total RNAs from cells by using TRIzol Reagent (Invitrogen, Carlsbad, CA, USA) according to the manufacturer's instruction. PrimeScriptTM RT Master Mix (Perfect Real Time, RR036A, TaKaRa) was used to reverse transcript total RNA (2 μg) to cDNA. QRT-PCR was conducted by using TB Green Fast qPCR mix (TaKaRa, Japan) according to the manufacturer's instruction. The thermocycling conditions were as follows: initial denaturation at 95 °C for 30 s; followed by 40 cycles of denaturing at 95 °C for 5 s, annealing and extension at 60 °C for 34 s. All reactions were conducted in triplicates. The relative gene expression was calculated by using $2^{-\Delta\Delta Ct}$ method. Human GAPDH gene was used as an endogenous control to normalize the data. RT-PCR primers for IL-6, NFKBIA and GAPDH are shown in Table S1.

Cell proliferation assay

The cell growth rate was determined by MTT assay. Cells at a density of 2–3 × 10^3 per well were added to 48-well plates in sixtuplicate and cultured in RPMI-1640 medium with 10% FBS. Following incubation for 4–5 days, 30 μL of fresh 0.5 mg/mL MTT reagent was added to each well and incubated for another 3–4 h. After incubation, 300 μL of DMSO was added to dissolve the formazan product and absorbance at 490 nm was then measured with SpectraMax iD3 (MD, USA).

Colony formation assay

A thousand cells were plated into each well in 6-well plate in triplicate with RPMI-1640 medium containing 10% FBS. The cells were cultured in an incubator (37 °C, 5% CO_2) for 7–10 days. The visible colonies were washed with phosphate-buffered saline (PBS), fixed with pre-cooled 4% paraformaldehyde for 10 min and then washed with PBS again. Finally, the colonies were stained with 0.5% crystal violet solution for 10 min, and washed with PBS for 3–5 times. Colony area was calculated by Image J software.

Wound healing assay

Cells at a density of 3–5 × 10^5 per well were seeded into 6-well plates and allowed to attain confluent monolayers. The cells were then

cultured in RPMI-1640 medium with 2% FBS for 12 h. Draw a line or a shape of " # " at the center of each well using a 10 μL pipette tip to create the wound area. The cells were washed with PBS twice to remove the deciduous cells. The cells were incubated for 48 h with RPMI-1640 medium supplemented with 2% FBS. When the cell wound almost healed, pictures (× 100) were taken and evaluating the effects of NFKBIA knockdown on cell migration.

Cell cycle analysis

The collected cells were fixed with 75% ethanol at −20 °C for 6 h or overnight, and then washed with pre-cooled PBS twice. The cells were stained with PI/Rnase Staining Buffer (BD Biosciences) and incubated at 37 °C for 10 min. Finally, the cell cycle was analyzed by FACS Calibur Flow Cytometer (BD Biosciences). The data was processed by FlowJo 10 software.

Western blotting analysis

The cells were lysed with RIPA buffer (Boster, China) containing protease/phosphatase inhibitor Cocktail (Boster, China). Total proteins from cultured cells were isolated and the concentrations were measured by the Bradford protein assay kit (Bio-Rad, Hercules, CA). After 10–12% SDS-PAGE, the proteins were electrotransferred to PVDF membrane (Bio-Rad). Then, membranes were blocked with 5% Nonfat Milk in Tris Buffered Saline (TBS) with 1‰Tween 20 (1 × TBST) for 90 min at room temperature. Next, the membranes were incubated with primary antibody in TBST overnight at 4 °C, followed by incubation with appropriate horseradish peroxidase (HRP)-conjugated secondary antibody (x 4000) for 1 h at room temperature. Specific proteins were detected with EZ-ECL Kit (Biological Industries). Primary antibodies from Cell Signaling Technology, Proteintech (Anti-Lamin B1) and abcam (Anti-QKI-5) were diluted 1000 times. Primary antibody from Santa Cruz Biotechnology (Anti-p65) was diluted 500 times.

Cytosol and nuclear protein extraction

The cells with 90% confluence in the dish were collected by using Nuclear and Cytoplasmic Protein Extraction Kit (Sangon Biotech, Shang hai) according to the manufacturer's instruction. The target protein expressions in cytoplasmic and nucleus were detected by Western Blot analysis. Lamin B1 was used as an internal control of nuclear protein, and GAPDH was used as an internal control of cytoplasmic protein.

Luciferase reporter assay

To determine whether miR-196b directly targets the 3′UTRs of *NFKBIA*, 5×10^4 293T cells were seeded in 24-well plates. Next day, miR-196b mimic (Thermo Scientific) plus empty 3′UTR vector or 3′UTR vectors containing WT or mut-3′UTR were transfected into the 293T cells. After 36 h, the cells were lysed and luciferase activity was measured by using Dual Luciferase Assay (Promega) according to the manufacturer's instructions.

RNA-binding protein immunoprecipitation (RIP) assay

To investigate the interaction between QKI-5 and miR-196b-5p in lung cancer cells, RIP assay was conducted by using Magna RIP kit (Millipore) according to the manufacturer's instructions. In brief, the QKI-5 knockdown H1299 cells and control cells were scraped off with pre-cooled PBS and collected into a centrifuge tube. The supernatant was removed after centrifugation, and the cells were re-suspended by adding a cell-isometric RIP lysis buffer (Millipore) containing proteases and RNase inhibitors. Protein A/G Magnetic Beads were incubated overnight with 5 μg of rabbit monoclonal anti-QKI5 antibody. Normal rabbit IgG (Millipore) was used as negative control. The cell lysates were added to antibody-bead complexes and incubated overnight. The immune complexes and input were washed, eluted and treated with 150 μL proteinase K and digested at 55 °C for 30 min. Immunoprecipitated RNA was extracted with phenol/chloroform and purified with ethanol precipitation. Finally, RNAs were subjected to qRT-PCR using specific Taqman probes.

ELISA assay

The cells were cultured in 6-well plates at a density of 3–5 × 10^5 cells/well overnight. The cells were washed with PBS and incubated in FBS free medium for 48 h. After 48 h, the supernatants were collected for enzyme-linked immunosorbent assay (ELISA). The secretion level of IL-6 in supernatant was measured according to the manufacturer's instructions.

In vivo xenograft model

Five-week-old athymic BALB/c nu/nu female mice (15–17 g, $n = 10$) were obtained from Vital River Laboratories (Beijing, China). All the procedures on animals according to the Institutional Animal Care and Use Committee (IACUC) guidelines of Wenzhou Medical University (wydw2020–0347). Stable NFKBIA knockdown H1299 cells (H1299/shNFKBIA) and control H1299 cells (H1299/shCont) were harvested with 0.25% EDTA-trypsin, washed with PBS, and resuspended in Matrigel/RPMI-1640 medium (1:1). The cells were subcutaneously injected into the flanks of nude mice at a concentration of 5 × 10^6 cells per 100 μL. The mice were sacrificed according to the animal welfare operation requirements, and tumor tissues were excised and weighed for further experiments. In addition, tumor volume was determined by measuring length (L) and width (W), and calculating volume (V=0.5×L×W^2) at the specified time points.

Immunohistochemistry staining

The harvested tumor tissues were fixed in 10% formalin, treated and embedded in paraffin as blocks for storage. Tissue sections were incubated with primary antibody against Ki67 (1: 100) or CD31 (1: 200) at 4 °C overnight and then incubated with secondary antibody at room temperature for 1 hour. After washing the slides, 3, 3′-diaminobenzidine (DAB) was used for color rendering.

Patient samples

NSCLC tissues samples and corresponding normal adjacent tissues (NATs) (30 patients with NSCLC) were obtained from Zhoushan Hospital of Wenzhou Medical University between 2018 and 2019. NSCLC tissues and NATs from patients were immediately placed in liquid nitrogen within 2 h of surgical resection and then stored at −80 °C until further analysis. This study was approved by the Institutional Research Human Ethical Committee of the Wenzhou Medical University (2,018,029) for the use of clinical biopsy specimens. The clinicopathological characteristics of the patients were shown in Table S2.

TCGA dataset

We downloaded log-2 transformed level 3 data of miRNA-seq and RNA-seq from TCGA database on July 31, 2013. Differences in expression levels of NFKBIA between NSCLC tissues and NATs were calculated by Welch *t*-test. Correlation between miR-196b-5p expression and NFKBIA expression in lung adenocarcinoma (LUAD) and lung squamous cell carcinoma (LUSC) was calculated by pearson correlation analysis.

Statistical analysis

GraphPad Prism 7.0 (GraphPad Software, CA, USA) was used to

perform all statistical analysis. Data are represented as means ± SD, and statistical significance was calculated with unpaired *t*-test unless indicated otherwise. $p < 0.05$ was considered as statistically significant. Correlation between miRNA and its target gene was calculated by Pearson correlation analysis.

Results

NFKBIA is a direct target of miR-196b-5p

We recently showed that the tumor suppressor, QKI-5 bound to and negatively regulated miR-196b-5p expression in NSCLC. miR-196b-5p exerted its oncogenic function by directly targeting GATA6, TSPAN12 and FAS [18,19]. Using a RIP assay, we further validated that miR-196b-5p was enriched in RIP samples using the QKI-5 antibody compared with those in RIP samples using the IgG in lung cancer cells. Of note, miR-196b-5p expression was markedly reduced in QKI-5 knockdown RIP samples when compared with control RIP samples (Fig. 1A and 1B), suggesting binding between QKI-5 and miR-196b-5p in NSCLC cells. The QKI-5 siRNA used in this study has been proven showing stronger knockdown effect than another siRNA in our previous study [19]. To further investigate the oncogenic functions of miR-196b-5p in NSCLC, we performed Pearson correlation analyses using the TCGA LUAD data set ($n = 487$) for previously reported 43 putative miR-196b-5p target genes [19]. Of these, 9 target genes showed significant negative correlation with miR-196b-5p, including NFKBIA, GATA6, TSPAN12 and FAS (Table 1). Since NFKBIA was a negative regulator of NF-κB and a novel potential target of miR-196b-5p, we selected NFKBIA for further analysis. Bioinformatics showed the 3′UTR of NFKBIA had a well conserved binding site for miR-196b-5p (Fig. 1C). To analyze this, we mutated the 3′UTR of NFKBIA at miR-196b-5p binding sites using the QuickChange Mutagenesis kit. Luciferase reporter assays showed that the miR-196b-5p significantly inhibited the luciferase activity of 3′UTR of NFKBIA in 293T cells when compared with empty vector. Co-transfection of miR-196b-5p with a mutated 3′UTR significantly attenuated the inhibition of luciferase activity on the wild type NFKBIA 3′UTR (Fig. 1D), suggesting specific binding between miR-196b-5p and NFKBIA 3′UTR. In addition, miR-196b-5p overexpression (Fig. 2A and 2B) significantly reduced both NFKBIA mRNA and protein levels in H1299 and A549 cells (Fig. 2C–2E). Conversely, knocking down miR-196b-5p partly but consistently increased both NFKBIA mRNA and protein levels (Fig. 2F-2H), indicating that NFKBIA might be a direct target of miR-196b-5p.

NFKBIA expression was down-regulated in NSCLC

We analyzed *NFKBIA* expression in NSCLC using TCGA LUAD (515 LUAD patients and 59 matched NATs) and LUSC dataset (502 LUSC patients and 51 matched NATs). The results showed that *NFKBIA* expression was significantly down-regulated in both LUAD ($p = 4.41e-12$) and LUSC ($p < 2.2e-16$) (Fig. 3A and 3B). We further analyzed *NFKBIA* expression in 30 NSCLC tissues and 30 NATs from Zhoushan Hospital of Wenzhou Medical University. Consistent with TCGA dataset, *NFKBIA* expression was significantly downregulated in NSCLC tissues compared with those in NATs ($p = 3.96e-07$) (Fig. 3C). To investigate whether down-regulated *NFKBIA* expression was associated with up-regulated miR-196b-5p expression in NSCLC tissues, we conducted Pearson correlation analyses using TCGA LUAD ($n = 487$) and LUSC ($n = 235$) samples with *miR-196b-5p* and *NFKBIA* expression data. A significant negative correlation between miR-196b-5p and *NFKBIA* was observed in both LUAD ($R=-0.16$, $p = 0.004$) and LUSC ($R=-0.5$, $p = 2.8e-16$), suggesting that reduced expression of *NFKBIA* might be related to the upregulated expression of miR-196b-5p in NSCLC (Fig. 3D and 3E). Our recent study found that the QKI-5 expression was negatively correlated with the miR-196b-5p expression in NSCLC and up-regulated miR-196b-5p promoted the cell cycle in NSCLC cells [19]. As our results showed a significant negative correlation between miR-196b-5p and *NFKBIA* in NSCLC, we further investigated the correlation between *QKI-5* and *NFKBIA*. As expected, Pearson correlation analyses using the TCGA NSCLC dataset from the GEPIA website showed *QKI-5* was positively associated with *NFKBIA* ($R = 0.36$, $p<2.2e-16$) (Fig. 3F), indicating that QKI-5 mediated up-regulation of miR-196b-5p is closely involved with NFKBIA down-regulation in NSCLC. Also, GEPIA TCGA NSCLC dataset showed the cell cycle related genes, CDK4 was up-regulated, while CDKN1A (p21) was significantly down-regulated in NSCLC tissues (Fig. S1A and 1B). Moreover, Pearson correlation analyses showed *NFKBIA* was negatively associated with *CDK4,* whereas positively associated with *CDKN1A* in NSCLC (Fig. S2A and 2B), suggesting the critical functions of NFKBIA in cell cycle progression.

Knockdown of NFKBIA facilitated lung cancer cell proliferation, migration, colony formation and cell cycle

To investigate the biological functions of NFKBIA on lung cancer cells, we established stable NFKBIA knockdown H1299 and A549 cells by shRNA technique. Western blot and qRT-PCR analyses were conducted to measure the NFKBIA protein (Fig. 4A) and mRNA (Fig. 4B) expressions after knockdown. Knocking down NFKBIA significantly enhanced cell proliferative (Fig. 4C), migratory (Fig. 4D), and colony forming ability (Fig. 4E and 4F) of both H1299 and A549 cells. Cell cycle analysis showed that knocking down NFKBIA facilitated transition of G1 to S phase cell cycle in both H1299 (Fig. 5A and 5B) and A549 cells (Fig. 5C and 5D). Furthermore, knocking down NFKBIA in H1299 and A549 cells consistently changed cell cycle G1 phase related proteins, including cyclin D1, CDK4, CDK6, CDK inhibitor 1A (P21) and 2C (P18) (Fig. 5E). These results indicated that accelerated cell cycle by NFKBIA knockdown might be responsible to the increased lung cancer cell proliferative and colony forming ability.

Knockdown of NFKBIA promoted tumor growth in vivo

We showed that NFKBIA was implicated in lung cancer cell growth *in vitro*. To further understand the functions of NFKBIA in tumor growth *in vivo*, the stable NFKBIA knockdown H1299/shNFKBIA cells and control cells were subcutaneously injected into the flanks of nude mice. Knocking down NFKBIA significantly increased tumor weight and volume *in vivo* compared with that in control cells (Fig. 6A–6C). We confirmed that down-regulated NFKBIA mRNA expression in tumor tissues from H1299/shNFKBIA injected mice compared with those in tumor tissues from control cells injected mice (Fig. 6D). Immunohistochemical analyses showed that immunoreactivities for both Ki67 and CD31 were significantly increased in the tumor tissues derived from H1299/shNFKBIA injected mice (Fig. 6E and 6F), suggesting that down-regulated NFKBIA promoted lung cancer cell proliferation and angiogenesis *in vivo*.

Knockdown of NFKBIA promoted pSTAT3 expression by activating NF-κB signaling

We showed that miR-196b directly targeted NFKBIA and the expression of *NFKBIA* was significantly down-regulated in NSCLC. NFKBIA, also known as IκBα, is a member of IkBs that negatively regulates NF-κB signaling [15]. Thus, we examined whether p65, a member of NF-kB family, was activated after knocking down NFKBIA. NFKBIA was enriched in the cytoplasm and its expression was markedly reduced in NSCLC cells after knocking down NFKBIA. As expected, knockdown of NFKBIA promoted nuclear translocation of p65 in both H1299 and A549 cells compared with those in control cells (Fig. 7A and 7B). Accumulating evidences have suggested that p65 stimulates IL-6 mRNA expression by binding to its promoter region [20,21]. IL-6 is a pro-inflammatory cytokine and reportedly promotes various cancer progression by activating JAK2/STAT3 pathway [22]. Therefore, we

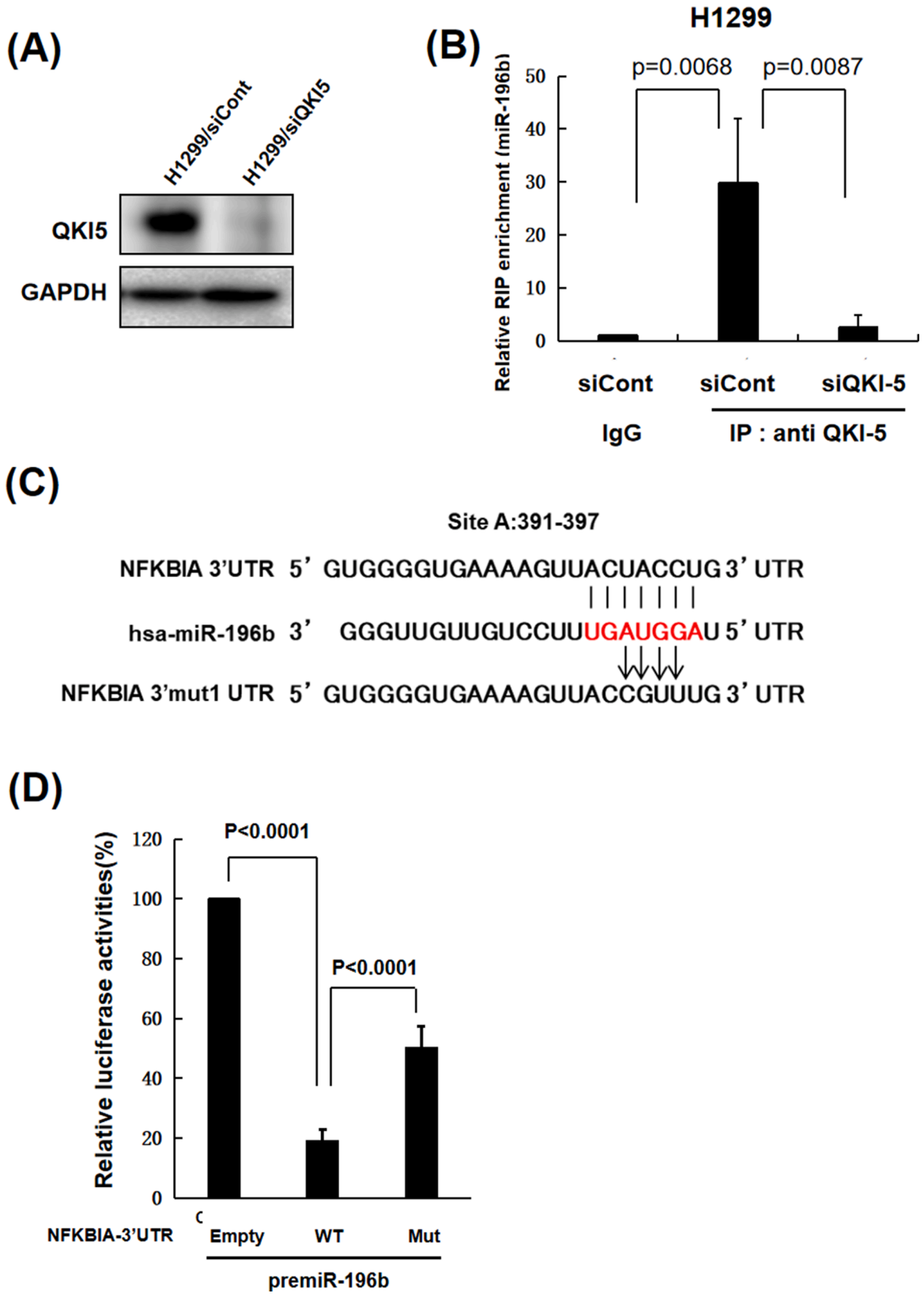

Fig. 1. NFKBIA is a direct target of miR-196b-5p. (A) Western blot analysis of QKI-5 in QKI-5 knockdown H1299 cells and control cells. GAPDH was used as an internal control. (B) Lysates from QKI-5 knockdown H1299 cells or control cells were subjected to RIP analysis. The cell extracts were subjected to immunoprecipitation with IgG or anti-QKI5 antibody. Pull-down RNA was analyzed by qRT-PCR using specific probe for miR-196b. Data are presented as mean ± SD as determined by triple assays. (C) Schematic diagram showing matched sequences between the seed sequence of miR-196b-5p and 3′UTRs of NFKBIA. The arrows indicate the mutagenesis nucleotides. (D) Luciferase reporter constructs containing wild-type, mutated form of NFKBIA 3′UTR, or empty vector were co-transfected with pre-miR-196b precursor into the 293T cells. Data are presented as mean ± SD as determined by triple assays. The *p*-values were calculated by one-way ANOVA with Tukey's multiple comparisons test. WT, wild-type; Mut, mutated form.

Table 1
Correlation analyses between miR-196b-5p and its target genes.

Target genes	Correlation coefficient	P-value
AQP4	−0.31	1.75E-12
ZC3H6	−0.28	3.70E-10
CCDC47	−0.21	3.68E-06
GATA6	−0.20	7.67E-06
TMEM161B	−0.17	1.37E-04
NFKBIA	−0.16	4.20E-04
SORCS1	−0.16	2.20E-03
TSPAN12	−0.15	7.69E-04
ZNF24	−0.13	4.20E-03
FAS	−0.14	2.50E-03

Table 1. Correlation between miR-196b-5p and its predicted target genes (http://mirwalk.umm.uni-heidelberg.de/) in TCGA lung ADC data set ($n = 487$).

investigated the expression of phosphorylated STAT3 (pSTAT3) in NFKBIA knockdown lung cancer cells. As shown in Fig. 7C and 7D, knocking down NFKBIA markedly increased the expression of pSTAT3. Next, we evaluated IL-6 mRNA and protein levels after knocking down NFKBIA. Knocking down NFKBIA markedly increased the expression of IL-6 mRNA and secreted protein levels in both H1299 (Fig. 7E and 7F) and A549 (Fig. 7G and 7H) cells. These results suggested that NFKBIA mediated activation of NF-κB increased pSTAT3 expression by promoting IL-6 secretion, resulted in facilitating lung cancer cell growth.

miR-224 down-regulated QKI-5 expression

Our previous research showed that miR-224 was significantly up-regulated in NSCLC, and exerted oncogenic functions in NSCLC [23,24]. Conversely, QKI-5 expression was down-regulated in NSCLC, and inhibited tumor progression in NSCLC [19]. Bioinformatics showed that the four of seven available miRNA target prediction websites predicted miR-224 directly targeting QKI-5 (Table S3). To investigate whether miR-224 influences QKI-5 and NFKBIA expressions, we overexpressed miR-224 in lung cancer cells (Fig. 8A). Overexpression of miR-224 partly reduced QKI-5 as well as NFKBIA protein expression levels in both H1299 and A549 cells (Fig. 8B and 8C). We further conducted Pearson correlation analysis to investigate the correlation between miR-224 and QKI-5 in NSCLC tissues. As expected, miR-224 was significantly anti-correlated with QKI-5 in NSCLC patient samples (correlation coefficient = −0.26, P = 4.28E-05, Fig. 8D), suggesting that up-regulated miR-224 reduced NFKBIA expression partly by targeting QKI-5 in NSCLC.

Discussion

Aberrant miRNA expression is frequently observed in NSCLC and is closely associated with disease progression and metastasis by regulating target gene expression [25]. MiR-196b functions are controversial in cancer. High expression is correlated with tumor size, tumor-node-metastasis stage, lymph node metastasis, and poor hepatocellular carcinoma prognosis by targeting SOCS2 [26]. In gastric cancer, miR-196b-5p expression is up-regulated, whereas its target gene, AQP4 is downregulated, suggesting disease promotion by directly targeting AQP4 [27]. Conversely, down-regulated miR-196b-5p is associated with metastases and poor outcomes in patients with colorectal cancer by influencing the expression of its target genes, HOXB7 and GALNT5 [28]. Our recent studies showed miR-196b-5p exerted oncogenic functions by directly targeting GATA6, TSPAN12, and FAS in NSCLC [18,19]. In the current study, we identified a novel direct target of miR-196b-5p, NFKBIA whose expression was negatively correlated with miR-196b-5p expression and was markedly downregulated in NSCLC tissues. Knocking down NFKBIA promoted cell proliferation, migration, colony formation, and cell cycle progression by activating NF-κB-mediated STAT3 signaling. We also showed that QKI-5 bound to and anti-correlated with miR-196b-5p in NSCLC. Additionally, we found that onco-miRNA, miR-224 negatively regulated QKI-5 expression, suggesting elevated miR-224 is closely associated with the down-regulated QKI-5 expression in NSCLC (Fig. 8E).

NF-κB signaling is constitutively activated in many cancer cells and causes abnormal cell growth and apoptosis evasion [29]. Under normal conditions, NF-κB remains inactive in the cytoplasm by IkB proteins, including NFKBIA. In response to external stimulation (viral and proinflammatory cytokines), activated IkB kinases (IKKs) phosphorylate IkBs, cause the ubiquitin-dependent degradation of IkBs, and facilitate the nuclear translocation of liberated NF-κB dimers [15,30]. In NSCLC, activated NF-κB signaling is closely associated with cell proliferation, apoptosis, angiogenesis, EMT, inflammation, and metastasis [31,32]. Activation of oncogenic K-rasG12D and the concomitant loss of p53 in a genetically engineered mouse model enhanced p65 nuclear translocation. Furthermore, the IkB-mediated suppression of NF-κB signaling reduced tumor development in a mouse model [33]. Here, we provided evidence showing that not only IKKs mediated IkBα phosphorylation, but also miR-196b-5p-mediated down-regulation of NFKBIA activated NF-κB signaling in NSCLC.

Activated NF-κB signaling promotes IL-6 secretion in the tumor microenvironment [34,35]. We recently showed that p65 overexpression increased IL-6 mRNA expression and protein secretion, which subsequently activated STAT3 signaling and enhanced lung cancer cell growth rates [18]. As expected, NFKBIA knockdown in NSCLC cells caused p65 nuclear translocation, suggesting activated NF-κB signaling in NSCLC. Further analyses showed NFKBIA knockdown increased pSTAT3 expression in NSCLC cells. To demonstrate IL-6 was a critical player in NFKBIA-mediated STAT3 activation, we investigated IL-6 expression levels after knocking down NFKBIA. NFKBIA knockdown in NSCLC cells increased both IL-6 mRNA expression and protein secretion, suggesting that NF-κB activation by NFKBIA inhibition increased pSTAT3 expression by enhancing IL-6 secretion.

Recently, several studies reported that some miRNAs directly targeted QKI-5 during cancer progression. MiR-221 overexpression enhanced tumorigenic capacity in colorectal carcinoma patient-derived xenografts cells *in vivo* by targeting QKI-5 [36]. Additionally, miR-200c regulated EMT-associated alternative splicing changes by targeting QKI-5, and this splicing signature was broadly conserved across many epithelial-derived cancer types [37]. He et al. reported that miR-143–3p suppressed cell proliferation and EMT by targeting QKI-5 in esophageal squamous cell carcinoma. However, the link between miR-224 and QKI-5 in cancer remains unclear. In the present study, miR-224 markedly down-regulated QKI-5 expression in NSCLC cells, and was anti-correlated with QKI-5 expression in tissues, suggesting down-regulated QKI-5 may be partly due to increased miR-224 expression in NSCLC.

Conclusions

In summary, we identified a novel target of miR-196b-5p, NFKBIA. MiR-196b-5p-mediated down-regulation of NFKBIA partly contributed to the NF-kB/IL-6 axis-mediated activation of STAT3 signaling. Also, miR-224 directly targeted QKI-5 in NSCLC. Therefore, targeting the miR-224/QKI-5/miR-196b-5p/NFKBIA pathway could be an effective therapeutic strategy for some NSCLC cases.

Funding

This work was supported by the National Natural Science Foundation of China (Grant No. 81672305), Natural Science Foundation of Zhejiang Province (Grant No. LZ22H160006), Health Commission of Zhejiang Province (Grant No. 2020RC136) and Key Laboratory of Clinical Laboratory Diagnosis and Translational Research of Zhejiang Province (Grant No. 2022E10022).

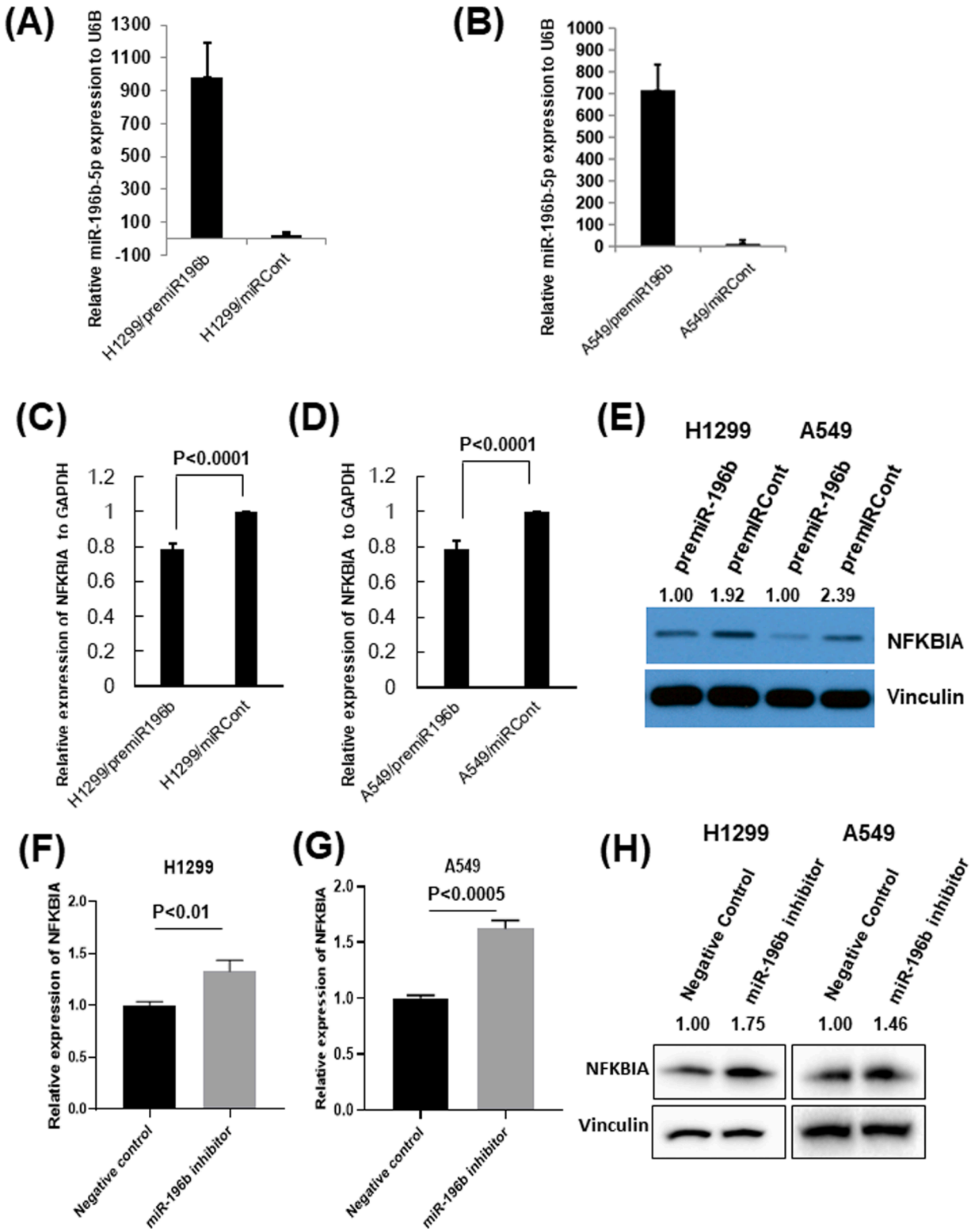

Fig. 2. Overexpression of miR-196b-5p downregulates the expression of NFKBIA. (A, B) qRT-PCR measures miR-196b-5p expression after overexpressing pre-miR-196b precursor in H1299 (A) and A549 (B) lung cancer cells. (C, D) qRT-PCR measures NFKBIA mRNA expression levels in H1299 (C) and A549 (D) lung cancer cells transfected with pre-miR-196b or control. (E) Western blot analyses measure NFKBIA protein levels in lung cancer cells (H1299 and A549) transfected with pre-miR-196b or control. (F, G) After transfection of anti-miR-196b, NFKBIA mRNA expression was measured by qRT-PCR in H1299 (F) and A549 (G) lung cancer cells. (H) After transfection of anti-miR-196b, NFKBIA protein expression was evaluated by western blot analyses. Data are presented as mean ± SD and *p*-values were calculated by unpaired *t*-test.

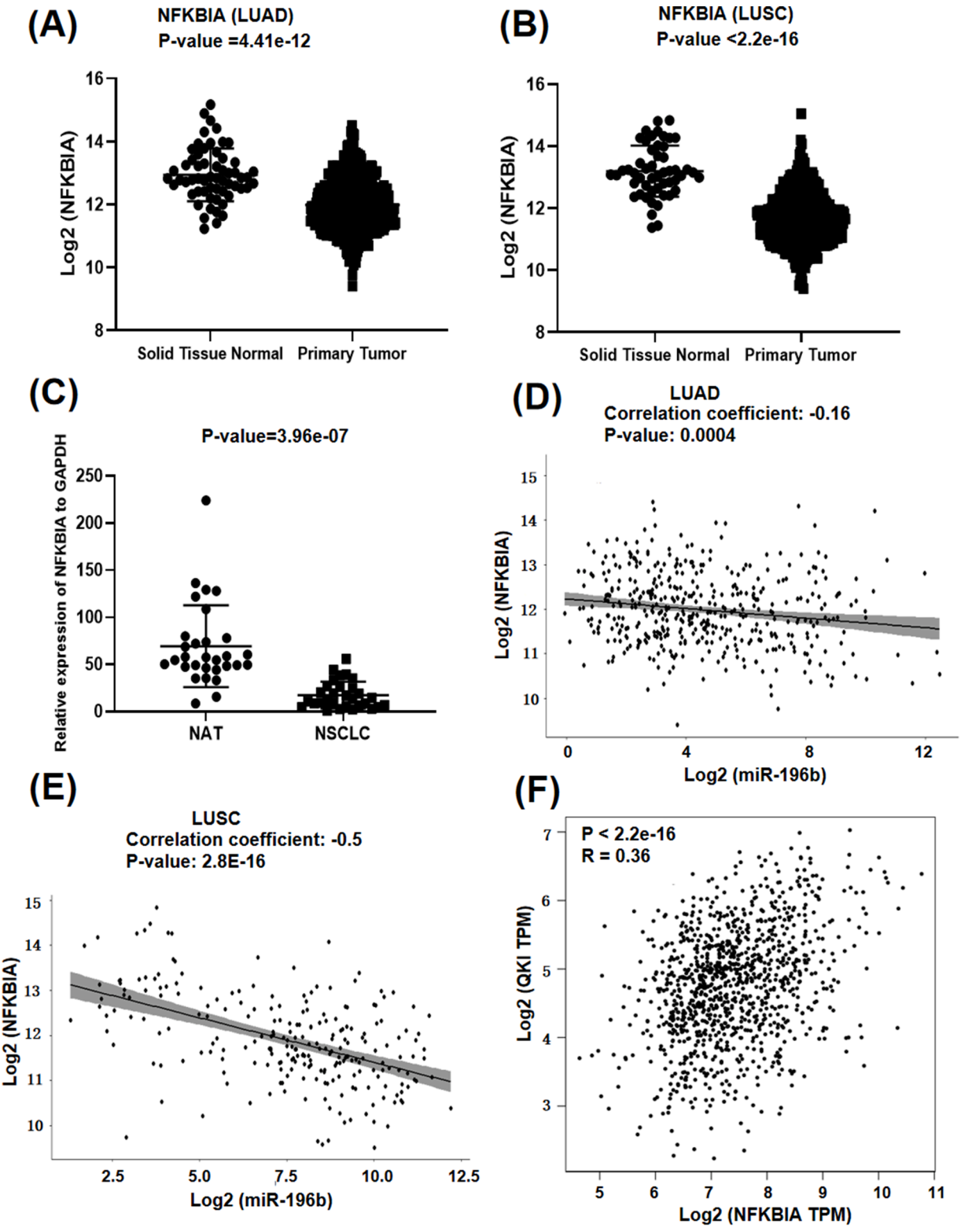

Fig. 3. NFKBIA is down-regulated in NSCLC. (A, B) The *NFKBIA* expression data were obtained from TCGA RNA-seq dataset. *NFKBIA* expressions were analyzed in 515 LUAD patients with 59 matched NAT samples (A) and 502 LUSC patients with 51 matched NAT samples (B). Welch *t*-test was conducted to calculate statistical significance. (C) Box plots showing the expression level of *NFKBIA* in 60 paired NSCLC tissues and their matched NATs. The RNA samples were extracted from 30 NSCLC tissues and 30 corresponding NATs. The RNAs were subject to qRT-PCR with an NFKBIA probe and the expression was normalized by GAPDH. (D, E) miR-196b-5p expression from miR-seq data and *NFKBIA* expression from TCGA RNA-seq data were used to examine correlation between *NFKBIA* and miR-196b-5p expressions in LUAD dataset ($n = 487$) (D) and LUSC dataset ($n = 235$) (E). (F) Correlation between *QKI* and *NFKBIA* in TCGA NSCLC RNA-seq data from GEPIA website. LUAD, lung adenocarcinoma; LUSC, lung squamous cell carcinoma; NAT, normal adjacent tissue. The *p*-values in (A-C) were calculated by unpaired *t*-test.

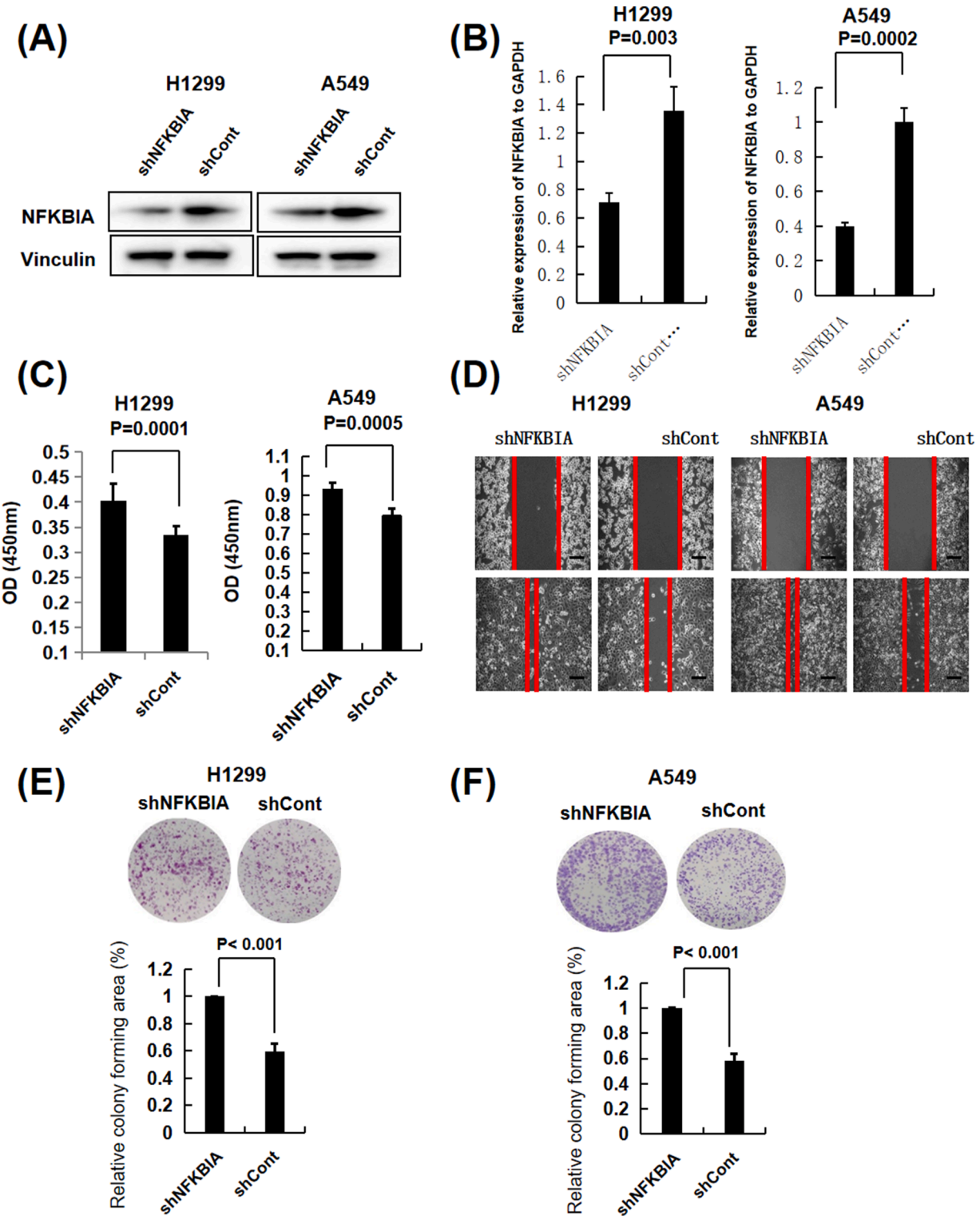

Fig. 4. Knocking down NFKBIA promotes lung cancer cell proliferation, migration and colony formation. (A, B) Western blot and qRT-PCR analyses of NFKBIA protein (A) and mRNA levels (B) in H1299 and A549 lung cancer cells transfected with shNFKBIA plasmids. GAPDH was used as an internal control. (C) Cell proliferation assay for NFKBIA knockdown H1299 and A549 lung cancer cells. The cell growth rates were measured by MTT assay. The values present mean ± SD as determined by sextuplet assays. (D) Representative pictures of wound healing assay for NFKBIA knockdown H1299 and A549 cells (× 100 magnification). (E, F) Colony formation assay for NFKBIA knockdown H1299 (E) and A549 (F) cells. Colony forming areas were measured by Image J software. The average values were derived from three random areas. Data are presented as mean ± SD and *p*-values were calculated by unpaired *t*-test.

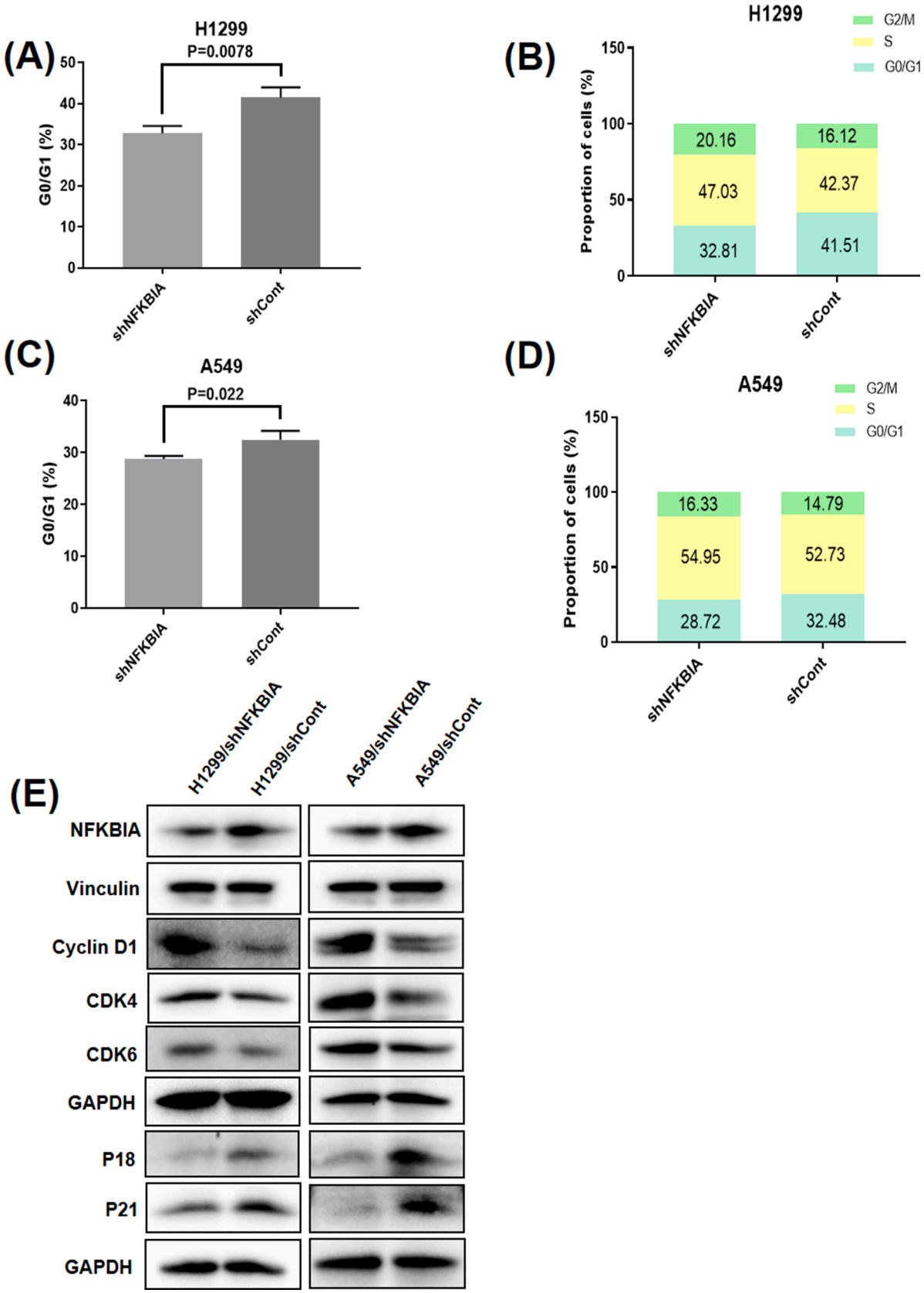

Fig. 5. Knocking down NFKBIA promotes cell cycle in NSCLC cells. (A, B) Proportion of cells in G0/G1 phase (A) and each cell-cycle phase (B) in H1299/shNFKBIA and H1299/shCont cells were determined by flow cytometry analysis. (C, D) Proportion of cells in G0/G1 phase (C) and each cell-cycle phase (D) in A549/shNFKBIA and A549/shCont cells were determined by flow cytometry analysis. (E) Western blot analysis of cell cycle G1 phase-related proteins (Cyclin D1, CDK4, CDK6, p18 and p21) in H1299/shNFKBIA, A549/shNFKBIA cells and corresponding control cells. GAPDH was used as an internal control. Data are presented as mean ± SD and *p*-values were calculated by unpaired *t*-test.

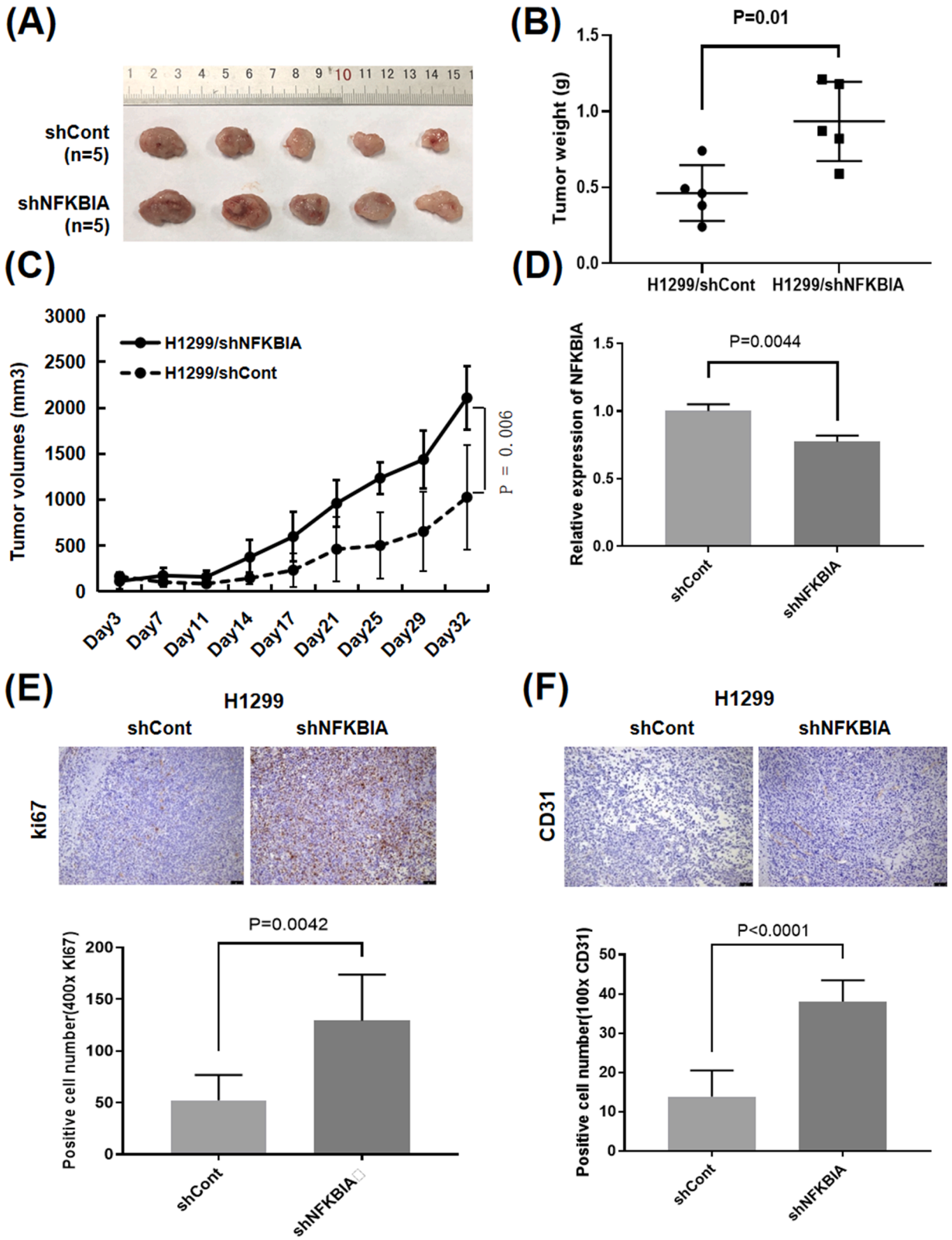

Fig. 6. Knocking down NFKBIA promotes tumor growth *in vivo*. (A-C) Effects of NFKBIA on tumor growth in mouse xenograft models. Representative photograph of tumors (A) and tumor weights (B) at day 33 after inoculation with either of the H1299/shNFKBIA or H1299/shCont cells. (C) Tumor growth in nude mice s.c. injected into flanks with H1299/shNFKBIA or H1299/shCont cells. Data are presented as mean ± SD ($n = 6$ per group). (D) NFKBIA mRNA expression in tumor tissues derived from H1299/shNFKBIA or H1299/shCont cells. The RNAs were extracted from tumor tissues and subject to qRT-PCR. The NFKBIA expression was normalized by GAPDH. (E, F) Ki67- (E) and CD31- (F) positive cells in tumors tissues derived from H1299/shNFKBIA or H1299/shCont cells. Paraffin sections of tumors developing in nude mice were stained with anti-Ki67 or anti-CD31 antibodies. The number of Ki67-positive tumor cells or CD31-positive microvessels in tumors that demonstrated the highest reactivities with antibodies were counted at × 400 or × 100, respectively, and presented as mean ± SD. The *p*-values were calculated by unpaired *t*-test.

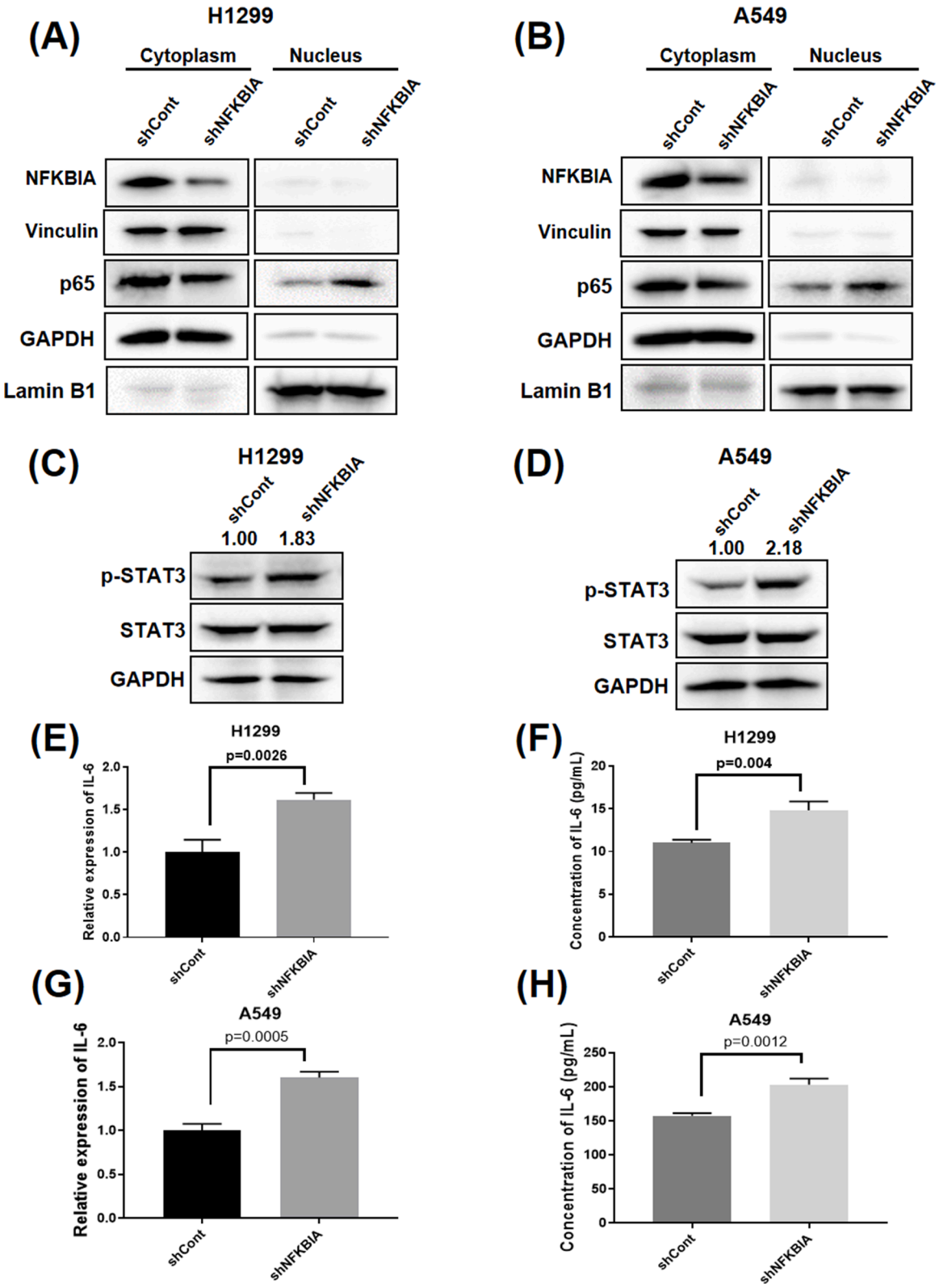

Fig. 7. Knocking down NFKBIA increases pSTAT3 expression by activating NF-κB signaling. (A, B) Western blot analysis of p65 protein in NFKBIA knockdown H1299 (A) and A549 (B) cells. Both nuclear and cytoplasm proteins were extracted and subjected to western blot analysis. Lamin B1 was used as a marker of nuclear protein, and GAPDH was used as a marker of cytoplasmic protein. (C, D) Western blot analysis to measure pSTAT3 and STAT3 protein expressions in H1299/shNFKBIA (C) and A549/shNFKBIA cells (D). GAPDH was used as an internal control. (E, F) qRT-PCR measures IL-6 mRNA expression (E) and ELISA analysis measures secreted IL-6 protein levels (F) in NFKBIA knockdown H1299 cells. (G, H) qRT-PCR measures IL-6 mRNA expression (G) and ELISA analysis measures secreted IL-6 protein levels (H) in NFKBIA knockdownA549 cells. Data are presented as mean ± SD and *p*-values were calculated by unpaired *t*-test.

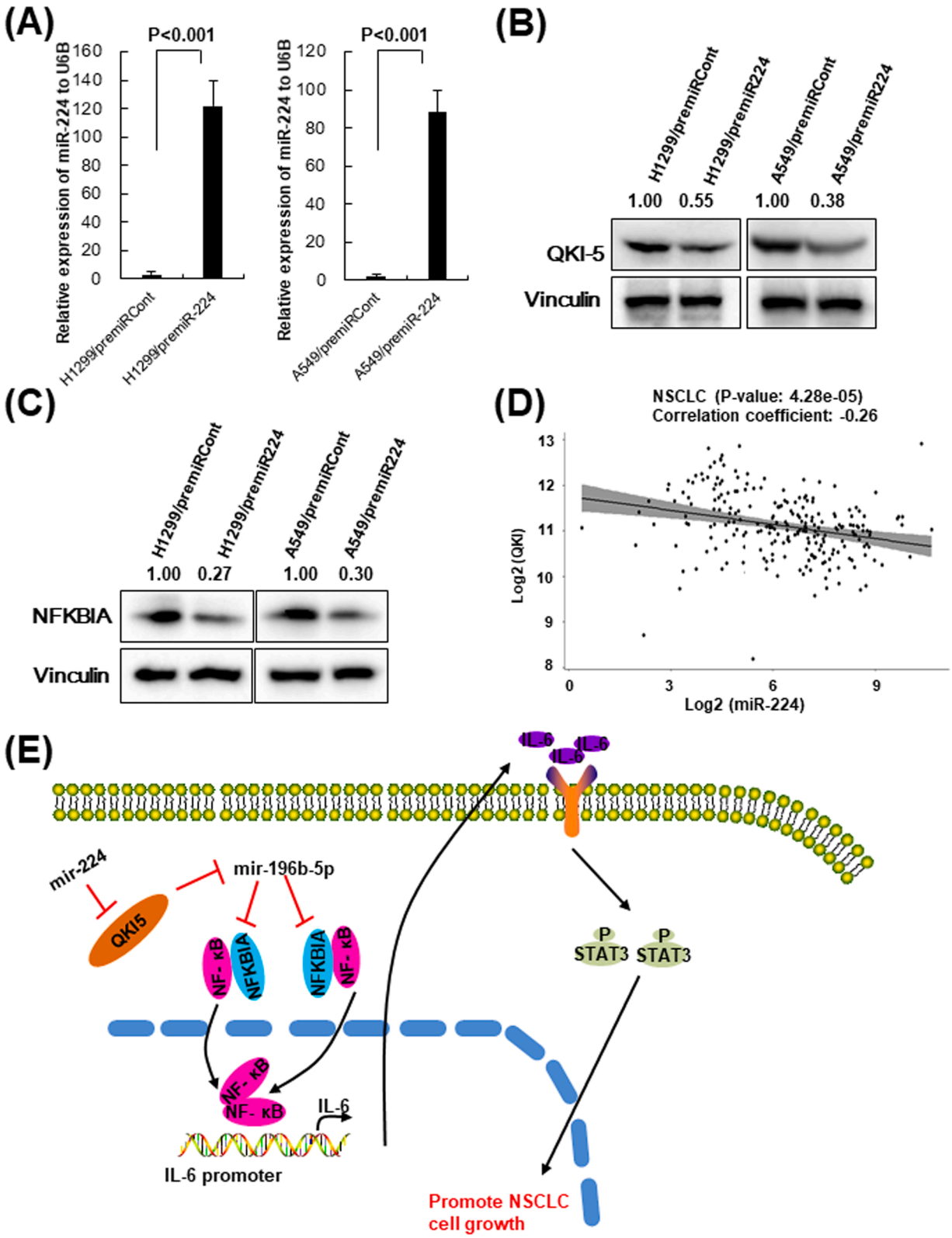

Fig. 8. Enhanced miR-224 is responsible for downregulated QKI-5 expression in NSCLC. (A) qRT-PCR measure miR-224 expression after overexpressing premiR-224 in H1299 and A549 cells. (B, C) Western blot analyses measure QKI-5 (B) and NFKBIA (C) protein expressions in H1299 and A549 cells after transfection with premiR-224 or control. (D) QKI expression from TCGA RNA-seq data and miR-224 expression from TCGA miR-seq data were used to examine the correlation between QKI and miR-224 expressions in LUSC dataset ($n = 235$). (E) Schematic Figure of proposed miR-196b-5p mediated down-regulation of NFKBIA increases pSTAT3 expression by activating NF-κB signaling. The *p*-values in (A) were calculated by unpaired *t*-test.

Ethics approval and patient consent statement

The study was conducted according to the guidelines of the Declaration of Helsinki, and approved by the Medical Research Ethics Committee and the Institutional Review Board of Wenzhou Medical University (approval number, 2,018,029). The informed consent was obtained from the all participated patients.

All animal studies were performed with an approved protocol by the Institutional Animal Care and Use Committee of Wenzhou Medical University (approval number, wydw2020–0347).

Consent for publication

All authors have agreed to submit this version of manuscript.

Availability of data and material

All data generated or analyzed during this study are included in this article. The datasets used and/or analyzed during the current study are available from the corresponding author on reasonable request.

CRediT authorship contribution statement

Wangyu Zhu: Data curation, Investigation, Methodology, Formal analysis, Resources, Funding acquisition, Validation, Visualization. **Yun Yu:** Data curation, Investigation, Methodology, Formal analysis, Software, Validation, Visualization. **Yuxin Ye:** Methodology, Formal analysis, Software. **Xinyue Tu:** Methodology, Formal analysis, Validation. **Yan Zhang:** Software, Validation. **Tao Wu:** Validation, Visualization. **Lianli Ni:** Validation. **Xiangjie Huang:** Validation. **Yumin Wang:** Funding acquisition, Writing – original draft, Writing – review & editing. **Ri Cui:** Conceptualization, Funding acquisition, Project administration, Supervision, Writing – original draft, Writing – review & editing.

Declaration of Competing Interest

The authors declare that they have no known competing financial interests or personal relationships that could have appeared to influence the work reported in this paper.

Acknowledgments

Not applicable.

Supplementary materials

Supplementary material associated with this article can be found, in the online version, at doi:10.1016/j.tranon.2023.101755.

References

[1] L. Osmani, F. Askin, E. Gabrielson, Q.K. Li, Current WHO guidelines and the critical role of immunohistochemical markers in the subclassification of non-small cell lung carcinoma (NSCLC): moving from targeted therapy to immunotherapy, Semin. Cancer Biol. 52 (Pt 1) (2018) 103–109, https://doi.org/10.1016/j.semcancer.2017.11.019.

[2] H. Sung, J. Ferlay, R.L. Siegel, M. Laversanne, I. Soerjomataram, A. Jemal, et al., Global cancer statistics 2020: GLOBOCAN estimates of incidence and mortality worldwide for 36 cancers in 185 countries, CA Cancer J. Clin. (2021) 209–249, https://doi.org/10.3322/caac.21660.

[3] R.L. Siegel, K.D. Miller, A. Jemal, Cancer statistics, CA Cancer J. Clin. 70 (1) (2020) 7–30, https://doi.org/10.3322/caac.21590.

[4] C.M. Croce, Causes and consequences of microRNA dysregulation in cancer, Nat. Rev. Genet. 10 (10) (2009) 704–714, https://doi.org/10.1038/nrg2634.

[5] G. Di Leva, M. Garofalo, C.M. Croce, MicroRNAs in cancer, Annu. Rev. Pathol. 9 (2014) 287–314, https://doi.org/10.1146/annurev-pathol-012513-104715.

[6] X. Xue, Y. Liu, Y. Wang, M. Meng, K. Wang, X. Zang, et al., MiR-21 and MiR-155 promote non-small cell lung cancer progression by downregulating SOCS1, SOCS6, and PTEN, Oncotarget 7 (51) (2016) 84508–84519, https://doi.org/10.18632/oncotarget.13022.

[7] J.G. Zhang, J.J. Wang, F. Zhao, Q. Liu, K. Jiang, G.H. Yang, MicroRNA-21 (miR-21) represses tumor suppressor PTEN and promotes growth and invasion in non-small cell lung cancer (NSCLC), Clin. Chim. Acta 411 (11–12) (2010) 846–852, https://doi.org/10.1016/j.cca.2010.02.074.

[8] U. Baumgartner, F. Berger, A. Hashemi Gheinani, S.S. Burgener, K. Monastyrskaya, E. Vassella, miR-19b enhances proliferation and apoptosis resistance via the EGFR signaling pathway by targeting PP2A and BIM in non-small cell lung cancer, Mol. Cancer 17 (1) (2018) 44, https://doi.org/10.1186/s12943-018-0781-5.

[9] D.H. Peng, S.T. Kundu, J.J. Fradette, L. Diao, P. Tong, L.A. Byers, et al., ZEB1 suppression sensitizes KRAS mutant cancers to MEK inhibition by an IL17RD-dependent mechanism, Sci. Transl. Med. 11 (483) (2019), https://doi.org/10.1126/scitranslmed.aaq1238.

[10] S.T. Kundu, L.A. Byers, D.H. Peng, J.D. Roybal, L. Diao, J. Wang, et al., The miR-200 family and the miR-183~96~182 cluster target Foxf2 to inhibit invasion and metastasis in lung cancers, Oncogene 35 (2) (2016) 173–186, https://doi.org/10.1038/onc.2015.71.

[11] M.A. Cortez, C. Ivan, D. Valdecanas, X. Wang, H.J. Peltier, Y. Ye, et al., PDL1 Regulation by p53 via miR-34, J. Natl. Cancer Inst. 108 (1) (2015), https://doi.org/10.1093/jnci/djv303.

[12] D.S. Hong, Y.K. Kang, M. Borad, J. Sachdev, S. Ejadi, H.Y. Lim, et al., Phase 1 study of MRX34, a liposomal miR-34a mimic, in patients with advanced solid tumours, Br. J. Cancer 122 (11) (2020) 1630–1637, https://doi.org/10.1038/s41416-020-0802-1.

[13] M. Karin, A. Lin, NF-kappaB at the crossroads of life and death, Nat. Immunol. 3 (3) (2002) 221–227, https://doi.org/10.1038/ni0302-221.

[14] X. Dolcet, D. Llobet, J. Pallares, X. Matias-Guiu, NF-kB in development and progression of human cancer, Virchows Arch. 446 (5) (2005) 475–482, https://doi.org/10.1007/s00428-005-1264-9. : an international journal of pathology.

[15] M. Karin, Y. Ben-Neriah, Phosphorylation meets ubiquitination: the control of NF-[*kappa*]B activity, Annu. Rev. Immunol. 18 (2000) 621–663, https://doi.org/10.1146/annurev.immunol.18.1.621.

[16] B. Rayet, C. Gelinas, Aberrant rel/nfkb genes and activity in human cancer, Oncogene 18 (49) (1999) 6938–6947, https://doi.org/10.1038/sj.onc.1203221.

[17] P. Crepieux, H. Kwon, N. Leclerc, W. Spencer, S. Richard, R. Lin, et al., I kappaB alpha physically interacts with a cytoskeleton-associated protein through its signal response domain, Mol. Cell. Biol. 17 (12) (1997) 7375–7385, https://doi.org/10.1128/mcb.17.12.7375.

[18] X. Huang, S. Xiao, X. Zhu, Y. Yu, M. Cao, X. Zhang, et al., miR-196b-5p-mediated downregulation of FAS promotes NSCLC progression by activating IL6-STAT3 signaling, Cell Death Dis. 11 (9) (2020) 785, https://doi.org/10.1038/s41419-020-02997-7.

[19] G. Liang, W. Meng, X. Huang, W. Zhu, C. Yin, C. Wang, et al., miR-196b-5p-mediated downregulation of TSPAN12 and GATA6 promotes tumor progression in non-small cell lung cancer, Proc. Natl. Acad. Sci. U.S.A. 117 (8) (2020) 4347–4357, https://doi.org/10.1073/pnas.1917531117.

[20] J. Nan, Y. Wang, J. Yang, G.R. Stark, IRF9 and unphosphorylated STAT2 cooperate with NF-kappaB to drive IL6 expression, Proc. Natl. Acad. Sci. U.S.A. 115 (15) (2018) 3906–3911, https://doi.org/10.1073/pnas.1714102115.

[21] X. Wang, W. Sun, W. Shen, M. Xia, C. Chen, D. Xiang, et al., Long non-coding RNA DILC regulates liver cancer stem cells via IL-6/STAT3 axis, J. Hepatol. 64 (6) (2016) 1283–1294, https://doi.org/10.1016/j.jhep.2016.01.019.

[22] D.E. Johnson, R.A. O'Keefe, J.R. Grandis, Targeting the IL-6/JAK/STAT3 signalling axis in cancer, Nat Rev Clin Oncol 15 (4) (2018) 234–248, https://doi.org/10.1038/nrclinonc.2018.8.

[23] R. Cui, W. Meng, H.L. Sun, T. Kim, Z. Ye, M. Fassan, et al., MicroRNA-224 promotes tumor progression in nonsmall cell lung cancer, Proc. Natl. Acad. Sci. U.S.A. 112 (31) (2015) E4288–E4297, https://doi.org/10.1073/pnas.1502068112.

[24] Y.J. Jeon, T. Kim, D. Park, G.J. Nuovo, S. Rhee, P. Joshi, et al., miRNA-mediated TUSC3 deficiency enhances UPR and ERAD to promote metastatic potential of NSCLC, Nat. Commun. 9 (1) (2018) 5110, https://doi.org/10.1038/s41467-018-07561-8.

[25] X. Zhu, M. Kudo, X. Huang, H. Sui, H. Tian, C.M. Croce, et al., Frontiers of MicroRNA signature in non-small cell lung cancer, Front. Cell Dev. Biol. 9 (2021), 643942, https://doi.org/10.3389/fcell.2021.643942.

[26] W. Ren, S. Wu, Y. Wu, T. Liu, X. Zhao, Y. Li, MicroRNA-196a/-196b regulate the progression of hepatocellular carcinoma through modulating the JAK/STAT pathway via targeting SOCS2, Cell Death Dis. 10 (5) (2019) 333, https://doi.org/10.1038/s41419-019-1530-4.

[27] J. Li, L. Wang, F. He, B. Li, R. Han, Long noncoding RNA LINC00629 restrains the progression of gastric cancer by upregulating AQP4 through competitively binding to miR-196b-5p, J. Cell. Physiol. 235 (3) (2020) 2973–2985, https://doi.org/10.1002/jcp.29203.

[28] V. Stiegelbauer, P. Vychytilova-Faltejskova, M. Karbiener, A.M. Pehserl, A. Reicher, M. Resel, et al., miR-196b-5p regulates colorectal cancer cell migration and metastases through interaction with HOXB7 and GALNT5, Clin. Cancer Res. 23 (17) (2017) 5255–5266, https://doi.org/10.1158/1078-0432.CCR-17-0023. : an official journal of the american association for, Cancer Res.

[29] M. Karin, Y. Cao, F.R. Greten, Z.W. Li, NF-kappaB in cancer: from innocent bystander to major culprit, Nat. Rev. Cancer 2 (4) (2002) 301–310, https://doi.org/10.1038/nrc780.

[30] Z.W. Li, W. Chu, Y. Hu, M. Delhase, T. Deerinck, M. Ellisman, et al., The IKKbeta subunit of IkappaB kinase (IKK) is essential for nuclear factor kappaB activation and prevention of apoptosis, J. Exp. Med. 189 (11) (1999) 1839–1845, https://doi.org/10.1084/jem.189.11.1839.

[31] W. Chen, Z. Li, L. Bai, Y. Lin, NF-kappaB in lung cancer, a carcinogenesis mediator and a prevention and therapy target, Front. Biosci. 16 (2011) 1172–1185, https://doi.org/10.2741/3782.
[32] C. Min, S.F. Eddy, D.H. Sherr, G.E. Sonenshein, NF-kappaB and epithelial to mesenchymal transition of cancer, J. Cell. Biochem. 104 (3) (2008) 733–744, https://doi.org/10.1002/jcb.21695.
[33] E. Meylan, A.L. Dooley, D.M. Feldser, L. Shen, E. Turk, C. Ouyang, et al., Requirement for NF-kappaB signalling in a mouse model of lung adenocarcinoma, Nature 462 (7269) (2009) 104–107, https://doi.org/10.1038/nature08462.
[34] B. Hoesel, J.A. Schmid, The complexity of NF-kappaB signaling in inflammation and cancer, Mol. Cancer 12 (2013) 86, https://doi.org/10.1186/1476-4598-12-86.
[35] M. Karin, Nuclear factor-kappaB in cancer development and progression, Nature 441 (7092) (2006) 431–436, https://doi.org/10.1038/nature04870.
[36] J. Mukohyama, T. Isobe, Q. Hu, T. Hayashi, T. Watanabe, M. Maeda, et al., miR-221 targets QKI to enhance the tumorigenic capacity of human colorectal cancer stem cells, Cancer Res. 79 (20) (2019) 5151–5158, https://doi.org/10.1158/0008-5472.CAN-18-3544.
[37] K.A. Pillman, C.A. Phillips, S. Roslan, J. Toubia, B.K. Dredge, A.G. Bert, et al., miR-200/375 control epithelial plasticity-associated alternative splicing by repressing the RNA-binding protein quaking, EMBO J. 37 (13) (2018), https://doi.org/10.15252/embj.201899016.